JOURNAL OF APPLIED POLYMER SCIENCE VOL. 20, 1555–1571 (1976)

Studies on Melt Spinning. VI. The Effect of Deformation History on Elongational Viscosity, Spinnability, and Thread Instability

CHANG DAE HAN and YOUNG WOO KIM, *Department of Chemical Engineering, Polytechnic Institute of New York, Brooklyn, New York 11201*

Synopsis

The effect of deformation history on the elongational behavior and spinnability of polypropylene melt was investigated by carrying out isothermal melt-spinning experiments. For the study, spinnerettes of different die geometries were used to investigate the effect, if any, of the entrance angle, the capillary length-to-diameter (L/D) ratio, and the reservoir-to-capillary diameter (D_R/D) ratio on the elongational behavior of molten threadlines. An experimental study was also carried out to investigate the phenomenon of draw resonance in the extrusion of polypropylene melts through spinnerettes of different die geometries. Draw resonance is the phenomenon which gives rise to pulsations in the threadline diameter when the stretch ratio is increased above a certain critical value. The results of our study show that the critical stretch ratio at which the onset of draw resonance starts to occur decreases as the L/D ratio is decreased, as the entrance angle is increased, as the D_R/D ratio is increased, as the melt temperature is decreased, and as the shear rate in the die is increased. Of particular interest is the observation that, at 180°C, the severity of fiber nonuniformity increases as the stretch ratio is increased, whereas at 200°C and 220°C, the severity of fiber nonuniformity first increases and then decreases as the stretch ratio is increased considerably above the critical value. A rheological interpretation of the observed onset of draw resonance is presented with the aid of the independently determined rheological data.

INTRODUCTION

It has been the practical experience of the fiber-producing industry that a slight change in spinnerette hole geometry can sometimes affect the fiber-forming characteristics of macromolecules. This may be understandable in view of the fact that many fiber-forming materials exhibit viscoelastic behavior under practical spinning conditions. It is a well-established fact that fluids which possess the elastic property exhibit geometry-dependent flow properties. For instance, it is well documented in the literature that die swell ratio, defined as the ratio of extrudate diameter to capillary diameter (d_j/D), decreases as the capillary length-to-diameter (L/D) ratio is increased,[1–4] as the reservoir-to-capillary diameter (D_R/D) ratio is decreased,[5,6] and also as the die entrance angle α is decreased.[7,8]

On the other hand, theoretical progress in this area has been very slow. So far, no theoretical attempt has been successful in predicting, for instance, the dependence of the d_j/D ratio on the L/D ratio for viscoelastic fluids.

Today, the choice of die geometry for achieving the best spinnability is based on past experience. Since spinnability must be correlatable to a fundamental rheological property (or properties) of a fiber-forming material, it is of practical importance to investigate the effect of spinnerette geometry on the rheological properties of the material. The particular rheological property that is believed to be relevant to the fiber-spinning process is *elongational viscosity*.

In recent years, several research groups[9–15] have tried to determine the elongational viscosity experimentally, using fiber-spinning processes such as the wet-spinning process[9,10] and the melt-spinning process,[11–15] Chen et al.[13] report that the failure mechanism of a melt-spun fiber depends on how the material was deformed prior to its stretching. However, there has so far been little published in the literature dealing with the elongational flow behavior and spinnability of a fiber-forming material as affected by the history of its shear deformation. In view of the fact that many fiber-forming materials possess viscoelastic properties which depend on the deformation history, the authors have felt it important to experimentally investigate this effect.

In a previous paper, we presented some experimental evidence[16] of a phenomenon of melt flow instability occurring in melt spinning, namely, draw resonance. Draw resonance is the phenomenon which gives rise to pulsations in the threadline diameter when the take-up speed of the threadline exceeds a certain critical value. Some other revealing experimental studies are reported in the literature.[17–19]

Although, in our earlier study, we ascribed the occurrence of draw resonance to the elastic property of the melt being spun, we have more recently carried out a more exhaustive experimental investigation to better understand the rheological significance of its occurrence.

In this paper, we shall present our experimental results, describing how die geometry affects the critical stretch ratio at which draw resonance starts to occur. The geometrical variables investigated in the die design are the entrance angle α, the capillary length-to-diameter ratio L/D, and the reservoir-to-capillary diameter ratio D_R/D. We will also discuss how processing variables (e.g., melt temperature, shear rate in the die, and cooling method) affect the critical stretch ratio.

EXPERIMENTAL

The spinning apparatus and experimental procedure used are the same as described in an earlier paper by Han and Lamonte,[12] except for the spinnerettes used (see Fig. 1). The fibers emerge into an electrically heated chamber maintained at the same temperature as the melt. The isothermal chamber is approximately 6 in. long and has three glass windows to permit observation of the emerging threadlines. The fiber was therefore not cooled after exiting the spinnerette. In the present study, five spinnerettes, each having three holes, were used, and their dimensions and specifications are described in Table I. With these spinnerettes we studied (a) the effect of the L/D ratio, (b) the effect of the die entrance angle α, and (c) the effect of the D_R/D ratio, all on the elongational behavior, spinnability, and critical stretch ratio in the occurrence of draw resonance. Polypropylene (Exxon Chemical, Resin E115) was used for melt spinning throughout the entire experiment.

TABLE I
Dimensions of Spinnerettes Used

Spinnerette	A	B	C	D	E
α	60°	60°	60°	180°	180°
D, mm	1.0	1.0	1.0	1.0	1.0
D_R, mm	4.0	4.0	4.0	4.0	8.0
L, mm	0.0	1.0	4.0	1.0	1.0
L/D	0.0	1.0	4.0	1.0	1.0
D_R/D	4.0	4.0	4.0	4.0	8.0

In the determination of elongational viscosity, measurements were taken of the fiber diameter by a photographic technique and of the fiber tension, by use of a Saxl tensiometer. Photographs of the fiber diameter were taken through glass windows in the isothermal chamber.

In the determination of the onset of draw resonance, motion pictures were taken of the molten threadline at various stretch ratios. Also, frozen fiber diameters were measured to determine their variation at various spinning conditions.

RESULTS AND DISCUSSION

Elongational Flow Behavior

In the determination of the apparent elongational viscosity, we have used the method of analyzing the melt-spinning data described in our earlier papers.[12,15]

Figure 2 gives a plot of apparent elongational viscosity versus elongation rate for polypropylene at 180°C when it was melt-spun through spinnerettes having different L/D ratios. Figure 2 shows that there is no evident influence of L/D ratio on the apparent elongational viscosity and that, for a given spinnerette, the correlation is independent of the stretch ratio V_L/V_0 used.

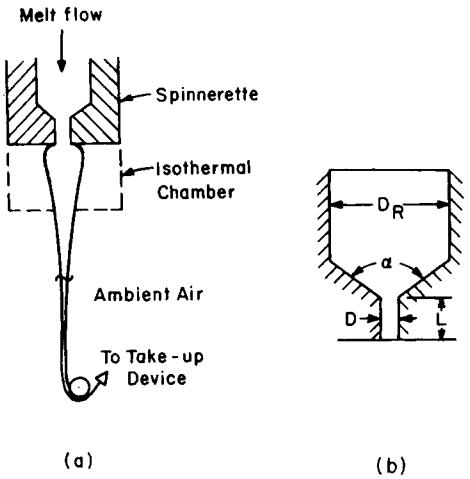

Fig. 1. Schematic of the spinning apparatus: (a) spinning line; (b) spinnerette geometry.

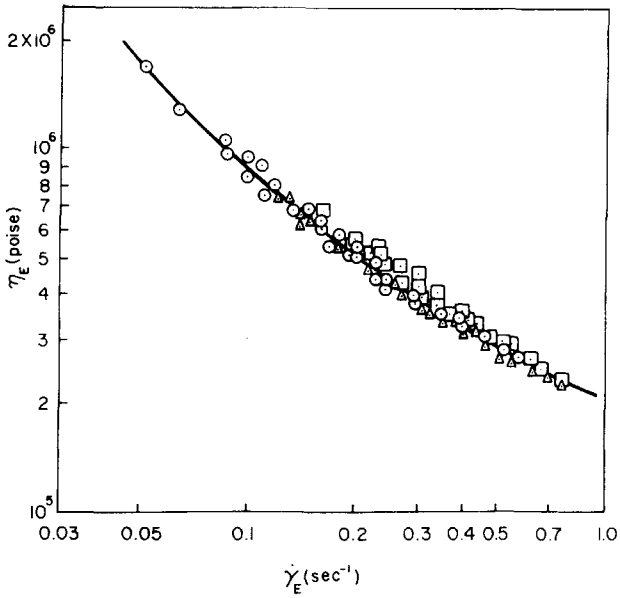

Fig. 2. Apparent elongational viscosity vs. elongation rate for spinnerettes of different L/D ratios: (⊙) L/D = 0 with stretch ratios of 41.6, 66.8, 75.1, 85.4, 104.3; (△) L/D = 1 with stretch ratios of 23.4, 36.0, 47.9, 64.9, 83.3; (□) L/D = 4 with stretch ratios of 23.8, 44.8, 56.3, 72.2, 98.6. Other die dimensions: $\alpha = 60°$, $D_R/D = 4$.

Figure 3 gives a plot of apparent elongational viscosity versus elongation rate for polypropylene at 180°C with spinnerettes having different D_R/D ratios. It is seen that the D_R/D ratio also does not seem to be an influencing factor on the apparent elongational viscosity. Note also that the data in Figure 3 were obtained at various stretch ratios.

The experimental evidence that die geometry, both L/D ratio and D_R/D ratio, has little influence on the apparent elongational viscosity can be inter-

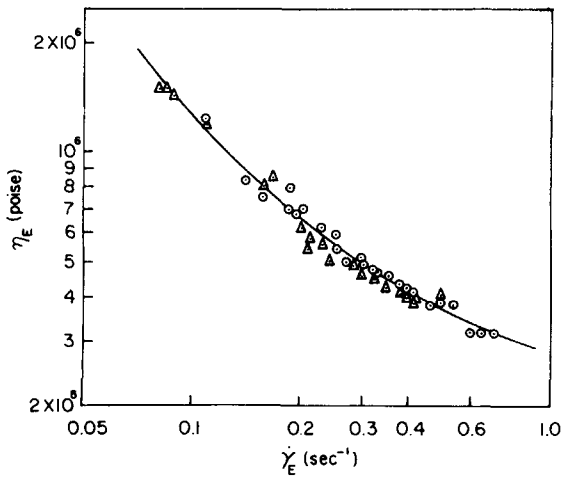

Fig. 3. Apparent elongational viscosity vs. elongation rate for spinnerettes of different D_R/D ratios: (⊙) D_R/D = 4 with stretch ratios of 26.8, 40.4, 46.5, 59.8, 69.4, 85.2; (△) D_R/D = 8 with stretch ratios of 20.3, 30.9, 40.3, 54.7, 61.7. Other die dimensions: $L/D = 1$, $\alpha = 180°$.

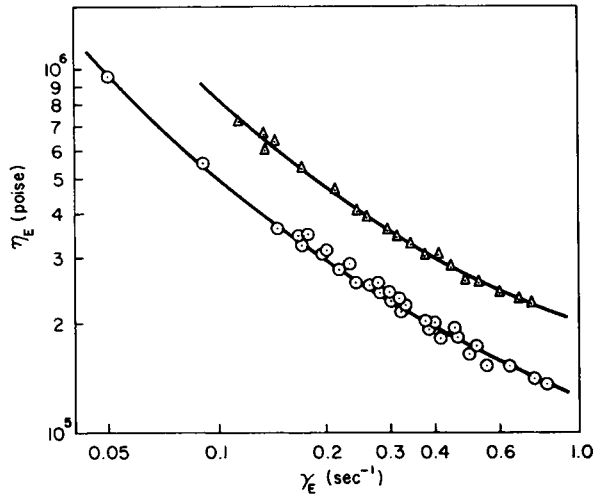

Fig. 4. Apparent elongational viscosity vs. elongation rate at two melt temperatures: (▲) 180°C with stretch ratios of 23.4, 36.0, 47.9, 64.9, 83.3; (⊙) 200°C with stretch ratios of 17.9, 27.2, 35.2, 45.6. The dimensions of the die used: $L/D = 1$, $\alpha = 60°$, $D_R/D = 4$.

preted as indicating that the measurements of apparent elongational viscosity were taken at positions where the influence of the shear deformation history of the melt was virtually nonexistent.

Figure 4 gives plots of apparent elongational viscosity versus elongation rate at two different melt temperatures, 180°C and 200°C. It is seen that an increase in melt temperature decreases the magnitude of elongational viscosity, as expected.

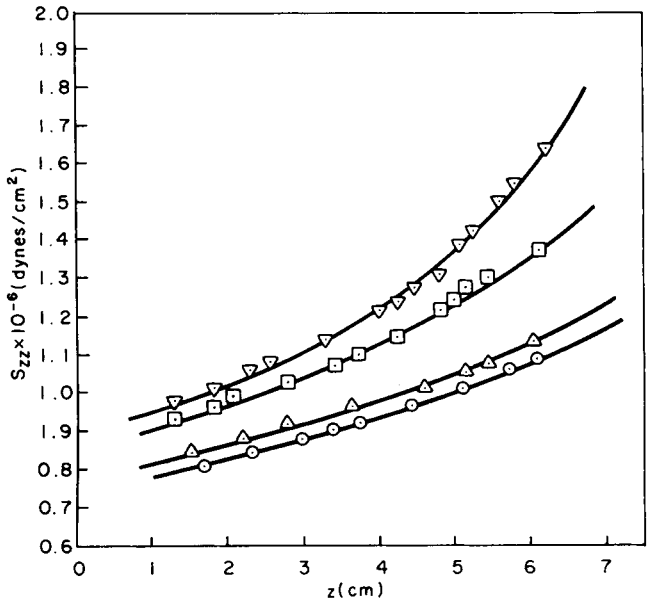

Fig. 5. Tensile stress vs. spinning way at various stretch ratios: (⊙) 23.4; (▲) 36.0; (⊡) 47.9; (▼) 64.9. Die dimensions: $L/D = 1$, $\alpha = 60°$, $D_R/D = 4$. Melt temperature: 180°C.

Figure 5 shows plots of tensile stress versus distance along the spinning way of an elongating filament at various stretch ratios. It is seen that the tensile stress increases with distance, for a fixed value of stretch ratio, and it increases with stretch ratio at a fixed position z. The increase in tensile stress along the spinning way notwithstanding, the apparent elongational viscosity has been found to decrease along the spinning way inside the *isothermal* chamber, almost independently of stretch ratio. This then indicates that, in the *absence* of thread cooling, the increase in elongation rate dv_z/dz along the spinning way is much greater than the increase of tensile stress S_{zz}, since the apparent elongational viscosity is defined by

$$\eta_E = \frac{S_{zz}}{(dv_z/dz)}. \tag{1}$$

In view of the fact that both tensile stress S_{zz} and elongation rate dv_z/dz vary along the flow direction z, the apparent elongational viscosity η_E determined from the melt-spinning experiment is a rheological property which also varies along the spinning way. It should be pointed out, therefore, that such a rheological property should be distinguished from the so-called *steady* elongational viscosity, where the elongation rate dv_z/dz is constant, i.e., independent of the flow direction z. Furthermore, the elongational viscosity determined under *steady* elongational flow should be independent of the direction of stretching.

Onset of Draw Resonance as Affected by Shear Deformation History

As reported in the literature,[16–19] draw resonance is the phenomenon in which the extruded thread exhibits pulsation of diameter when the stretch ratio is increased above a certain critical value. The severity of thread pulsation then increases as the stretch ratio is further increased beyond the critical value, ultimately leading to a breakdown of the threadline.

Figure 6 shows a typical plot of time versus the ratio of diameter-to-average diameter $d(t)/\bar{d}$ for a pulsing threadline at an apparent stretch ratio V_L/V_0 of 58.5. Note that Figure 6 was prepared from a series of motion pictures taken of the pulsing threadline by reading off the thread diameter from the projected image. It is seen that the thread diameter pulsates with a fre-

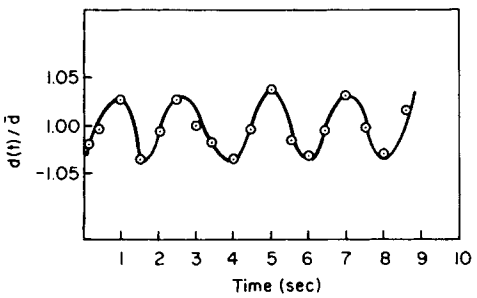

Fig. 6. Plots of time vs. the pulsing fiber diameter-to-average diameter ratio. Die dimensions: L/D = 0; D_R/D = 4; α = 60°. Stretch ratio V_L/V_0 = 58.5. Average fiber diameter $\bar{d}$ = 1.988 mm.

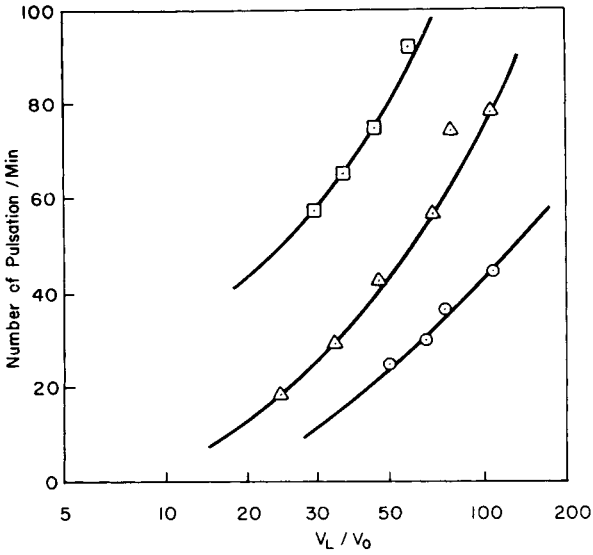

Fig. 7. Plots of the number of pulsations vs. apparent stretch ratio of a melt-spun threadline in the state of draw resonance at different melt temperatures: (⊡) T = 180°C; (△) T = 200°C; (⊙) T = 220°C. Spinnerette geometry: L/D = 1; D_R/D = 8; α = 180°. Spinning conditions: melt-spun into ambient air; shear rate in the spinnerette is approximately the same for all three temperatures, $\dot{\gamma}_{app} \approx 380\ \text{sec}^{-1}$.

quency and an amplitude whose values may depend on material characteristics and processing conditions.

Figure 7 shows plots of the pulsation frequency versus *apparent* stretch ratio V_L/V_0 at different melt temperatures. It is seen that thread pulsation increases with stretch ratio at a given melt temperature and that thread pulsation brings about an ultimate breakdown of the threadline.

Figure 8 gives typical plots of the ratio of minimum-to-maximum fiber diameter d_{min}/d_{max} versus *apparent* stretch ratio V_L/V_0. The diameters were determined from solidified fiber samples. Critical values of apparent stretch ratio $(V_L/V_0)_{crit}$ may be determined by extrapolating the curves in Figure 8 to yield $d_{min}/d_{max} = 1.0$. Of particular interest in Figure 8 is the observation

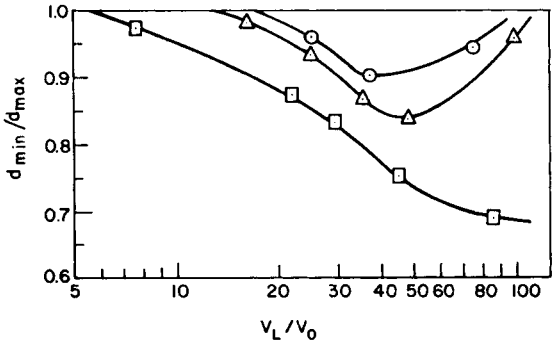

Fig. 8. Plots of the minimum-to-maximum diameter ratio of the melt-spun fibers vs. apparent stretch ratio at different melt temperatures: (⊡) T = 180°C; (△) T = 200°C; (⊙) T = 220°C. Spinnerette geometry: L/D = 1.0; D_R/D = 4; α = 60°.

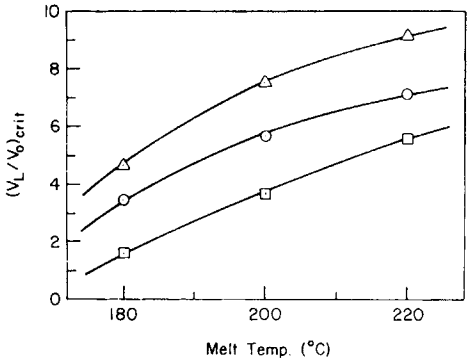

Fig. 9. Apparent critical stretch ratio vs. melt temperature in melt spinning for different values of L/D ratio: (▲) 4.0; (⊙) 1.0; (⊡) 0.0. Other die dimensions: $D_R/D = 4.0$; $\alpha = 60°$.

that, at 180°C, the severity of fiber nonuniformity increases as the stretch ratio is increased, whereas, at higher temperatures (200°C and 220°C), the severity of fiber nonuniformity first increases and then decreases as the stretch ratio is increased considerably above the critical value. In other words, it is possible to produce a more uniform fiber at stretch ratios very much above the onset point if the melt temperature (and possibly other processing variables as well) is properly chosen.

Figure 9 shows plots of *apparent* critical stretch ratio $(V_L/V_0)_{crit}$ versus melt temperature, and Figure 10 shows plots of *true* critical stretch ratio $(V_L/V_j)_{crit}$ versus melt temperature for three values of L/D ratio. Here, V_j is the thread velocity at the position where the maximum die swell occurs. Using the mass balance equation, one can calculate V_j by

$$V_j = V_0(D/d_j)^2 \tag{2}$$

where V_0 is the average velocity in the spinnerette hole, d_j is the relaxed thread diameter near the spinnerette, and D is the spinnerette hole diameter. In this study, d_j was determined by taking photographs of the molten threadline in the isothermal chamber (see Fig. 1).

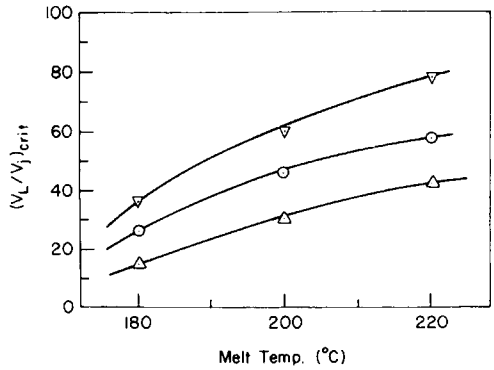

Fig. 10. True critical stretch ratio vs. melt temperature in melt spinning for different values of L/D ratio: (▼) 4.0; (⊙) 1.0; (▲) 0.0. Other die dimensions: $D_R/D = 4.0$; $\alpha = 60°$.

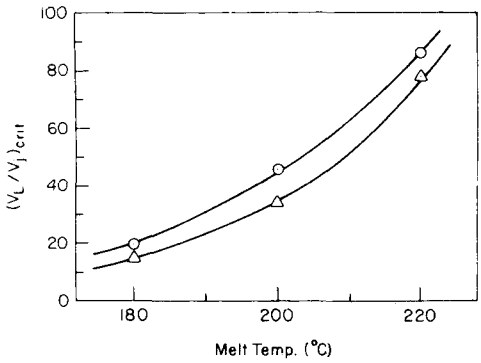

Fig. 11. True critical stretch ratio vs. melt temperature in melt spinning for different values of D_R/D ratio: (⊙) 4.0; (▲) 8.0. Other die dimensions: L/D = 1.0; α = 180°.

Two important observations may be made from Figures 9 and 10: (1) at a fixed value of L/D ratio, the critical stretch ratio is increased as the melt temperature is increased; (2) at a fixed melt temperature, the long die (i.e., the die having a large L/D ratio) gives rise to higher critical stretch ratios than the short die.

Figure 11 gives plots of $(V_L/V_j)_{crit}$ versus melt temperature for two values of D_R/D ratio. It is seen that the critical stretch ratio is increased as the D_R/D ratio is decreased from 8 to 4. It is also seen that, for a given die geometry, an increase in melt temperature brings about a higher critical stretch ratio, implying less thread pulsation.

Different methods of cooling the molten threadline are also seen to affect the critical stretch ratio and, therefore, the uniformity of threadlines. Figure 12 illustrates the effect of two different methods of cooling. A *delayed* quenching (i.e., the threadline first travels through an isothermal chamber and then into ambient air, as shown in Fig. 1) gives rise to higher values of critical stretch ratio and hence more uniform fiber than immediate quenching, in which the threadline passes directly into quiescent ambient air *without* passing through an isothermal chamber. This observation is consistent with the practical experience of commercial spinning operations.[20,21]

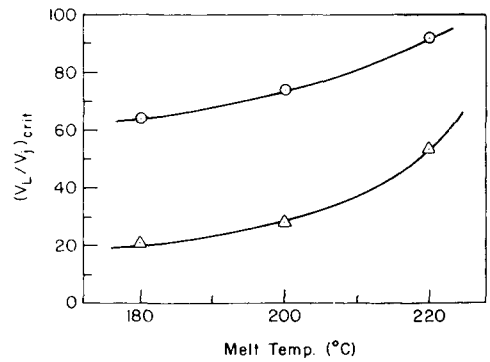

Fig. 12. True critical stretch ratio vs. melt temperature in melt spinning with different methods of cooling the fiber: (⊙) spun into an isothermal chamber with delayed quenching; (▲) spun directly into ambient air. Spinnerette geometry: D_R/D = 8.0; L/D = 1.0; α = 180°.

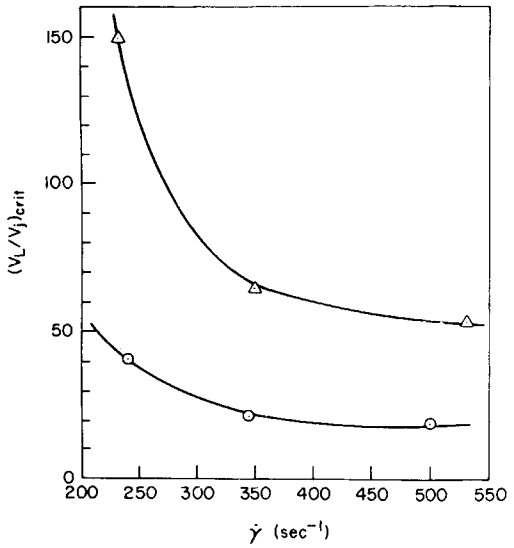

Fig. 13. True critical stretch ratio vs. apparent shear rate within the spinnerette hole: (▲) spun into an isothermal chamber with delayed quenching; (⊙) spun directly into ambient air. Spinnerette geometry: $D_R/D = 8$; $L/D = 0.0$; α 60°. Melt temperature = 180°C.

Figure 13 shows that the critical stretch ratio is decreased as the shear rate in the spinnerette hole is increased. This clearly indicates that the shear deformation history (in terms of the residence time that the fluid experienced) influences the onset of draw resonance.

Figure 14 gives a plot of the maximum stretch ratio $(V_L/V_0)_{max}$ versus shear rate in the spinnerette hole. Here, the maximum stretch ratios were determined from the experimentally measured pullaway speed (sometimes

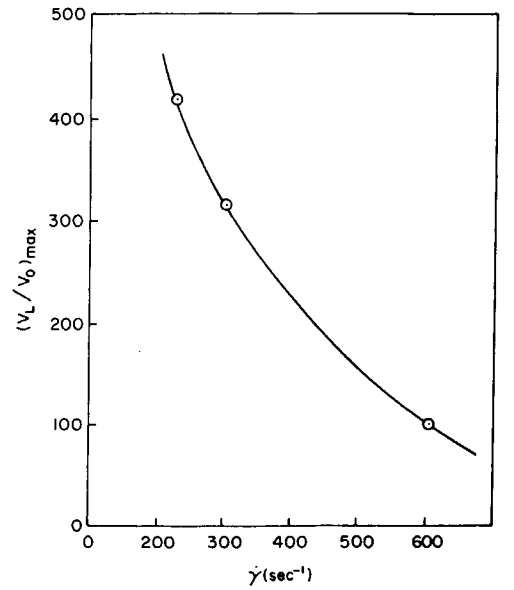

Fig. 14. Maximum stretch ratio vs. apparent shear rate within the spinnerette hole. Die geometry: $L/D = 1.0$; $D_R/D = 8.0$; $\alpha = 180°$. Melt temperature 180°C.

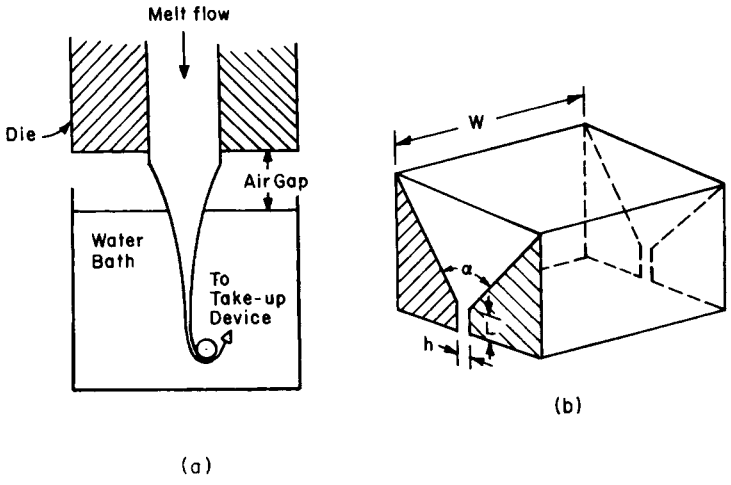

Fig. 15. Schematic of the film extrusion apparatus: (a) film line; (b) die geometry.

referred to as draw-down speed) at which a threadline first breaks. Although $(V_L/V_0)_{max}$ is not a rheological property, it is considered to be a useful parameter which can be used as a measure of the spinnability of fiber-forming materials.[12,15] One can then conclude from Figure 14 that the shear deformation history in the spinnerette definitely influences the spinnability of polypropylene.

At this point, it is interesting to review some recent experimental data of the onset of draw resonance in an entirely different polymer operation, namely, flat-film extrusion. Figure 15 is a schematic of the film extrusion apparatus, and Table II gives dimensions and specifications of the sheet-forming die used by Han and Funatsu.[22]

Figure 16 gives plots of *apparent* critical stretch ratio $(V_L/V_0)_{crit}$ versus melt temperature for different values of die land length (see Fig. 15b and Table II). It is seen that the critical stretch ratio is increased as the die land length (L/h ratio) is increased. Of course, an increase of die land length influences the shear deformation history of the melt. Figure 17 gives plots of apparent stretch ratio versus melt temperature for different die entrance angles (see Fig. 15b and Table II), in which it can be seen that the die having the smaller entrance angle α (20 degrees) gives rise to higher values of critical stretch ratio. In both Figures 16 and 17, the critical stretch ratio is increased as the melt temperature is increased. This observation is consistent with that made above with respect to melt spinning.

TABLE II
Dimensions of Flat-Film Dies Used

Film die	A	B	C	D	E	F	G	H
α, degrees	20	20	20	20	90	90	90	90
L, in.	0.0	0.040	0.100	0.400	0.0	0.040	0.100	0.400
h, in.	0.020	0.020	0.020	0.020	0.020	0.020	0.020	0.020
L/h	0	2	5	20	0	2	5	20

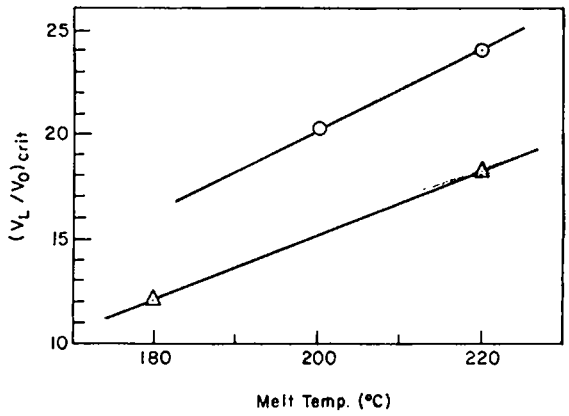

Fig. 16. Apparent critical stretch ratio vs. melt temperature in flat-film extrusion for different values of L/h ratio: (▲) 0.0; (⊙) 20.

Figure 18 gives plots of apparent critical stretch ratio versus shear rate in the sheet-forming die at two melt temperatures. It is seen again that the shear deformation history influences the onset of draw resonance in a manner very similar to that shown in Figure 13 for the melt-spinning experiment. In other words, both melt-spinning and flat-film extrusion processes give rise to similar results insofar as the effect of the shear deformation history on the onset of draw resonance is concerned.

It should be mentioned at this point that, from the practical standpoint, the calculation of $(V_L/V_j)_{crit}$ in flat-film extrusion is very difficult, if not impossible, because of the nonuniform swelling of the extrudate exiting from a noncircular die. Therefore, the average velocity in the die (hence, the apparent stretch ratio) was used in Figure 16 to 18. Consequently, the critical stretch ratios in flat-film extrusion given in these figures are much lower than

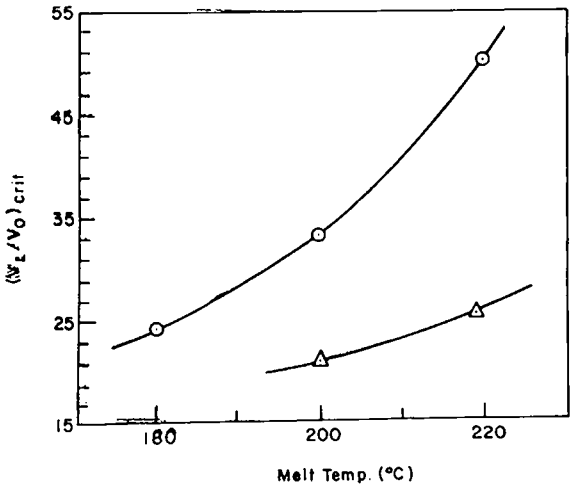

Fig. 17. Apparent critical stretch ratio vs. melt temperature in flat-film extrusion for different values of entrance angle: (⊙) 20°; (▲) 90°.

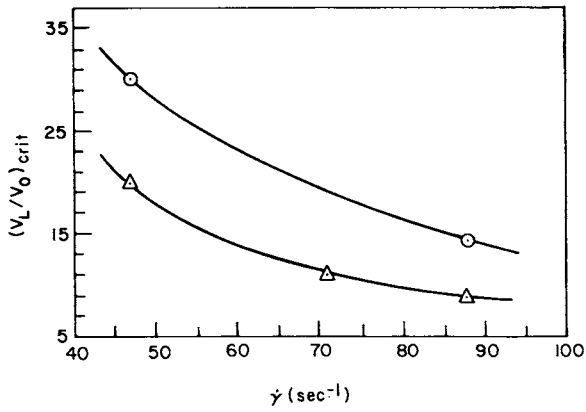

Fig. 18. Apparent critical stretch ratio vs. apparent shear rate within the film die for different melt temperatures: (▲) T = 180°C; (⊙) T = 200°C. Die geometry: L/h = 0.0; α = 20°.

those in melt spinning given in Figures 10 to 13, which are based on the true stretch ratio $(V_L/V_j)_{crit}$.

Rheological Interpretation of Draw Resonance

Today, it is a well-known fact that the recoverable elastic strain of a fluid decreases with temperature. Figure 19 shows plots of first normal stress difference $\tau_{11} - \tau_{22}$ versus shear rate $\dot{\gamma}$ for polypropylene melts at three temperatures, 180°, 200°, and 220°C. It is seen that $\tau_{11} - \tau_{22}$, which is a measure of fluid elasticity, decreases with temperature. Figure 20 shows plots of shear viscosity η versus shear rate $\dot{\gamma}$ at three temperatures, 180°, 200°, and 220°C, and it is seen that η also decreases as the temperature increases.

In view of the fact that the critical stretch ratio is increased as the melt temperature is increased (see Figs. 10 to 13), together with the fact that $\tau_{11} -$

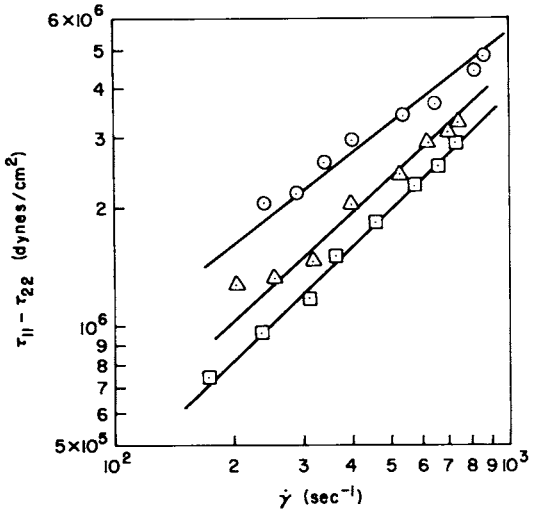

Fig. 19. Plots of first normal stress difference vs. shear rate for polypropylene at different melt temperatures: (⊙) T = 180°C; (▲) T = 200°C; (⊡) T = 220°C.

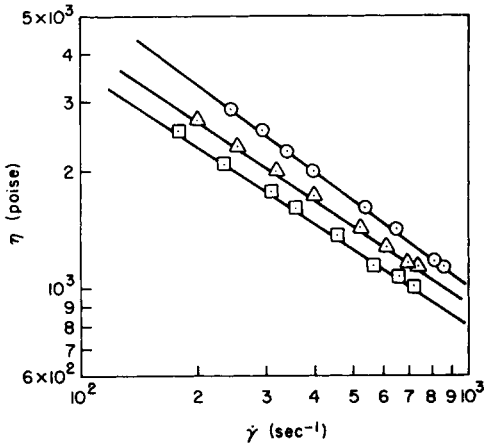

Fig. 20. Plots of shear viscosity vs. shear rate for polypropylene at different melt temperatures: (⊙) T = 180°C; (△) T = 200°C; (□) T = 220°C.

τ_{22} (and also die swell ratio) decreases as the melt temperature is increased (see Fig. 19), it may be concluded that the increase of critical stretch ratio in the occurrence of draw resonance may be attributable to the corresponding decrease of fluid elasticity (i.e., $\tau_{11} - \tau_{22}$ or d_j/D). It should be pointed out that the thread diameter becomes more uniform as the melt temperature is increased. This observation is consistent with that made by Bergonzoni and DiCresce,[19] who report that the amount of thread pulsing was lower as the melt temperature was increased.

It has been much discussed in the literature[1-8] that melt elasticity (in terms of die swell ratio) depends on die geometry. Furthermore, it is found that the recoverable elastic strain of a polymer melt decreases as the L/D ratio is increased (Fig. 21, from ref. 4) and also as the D_R/D ratio is decreased (Fig. 22, from ref. 6). Therefore, it can be concluded that the observed in-

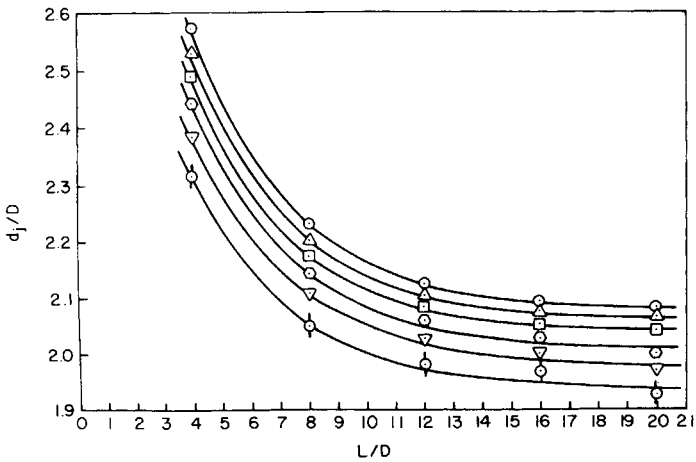

Fig. 21. Plots of die swell ratio vs. L/D ratio for high-density polyethylene at 180°C for different values of shear rate[4]: (⊙) $\dot{\gamma}$ = 700 sec^{-1}; (△) $\dot{\gamma}$ = 600 sec^{-1}; (□) $\dot{\gamma}$ = 500 sec^{-1}; (⊙) $\dot{\gamma}$ = 400 sec^{-1}; (▽) $\dot{\gamma}$ = 300 sec^{-1}; (◇) $\dot{\gamma}$ = 200 sec^{-1}.

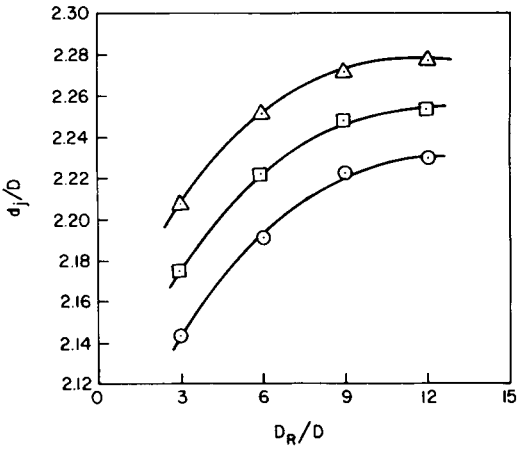

Fig. 22. Plots of die swell ratio vs. D_R/D ratio for high-density polyethylene at 180°C for different values of shear rate[6]: (△) $\dot{\gamma} = 400\ \text{sec}^{-1}$; (□) $\dot{\gamma} = 350\ \text{sec}^{-1}$; (○) $\dot{\gamma} = 300\ \text{sec}^{-1}$.

crease in the critical stretch ratio as the L/D ratio is increased (and as the D_R/D ratio is decreased) may be attributable to the corresponding decrease in the amount of recoverable elastic strain of the melt upon exiting from the die. In other words, the onset of draw resonance may be related to the elastic properties of the exiting melt.

Some attempts at explaining the occurrence of draw resonance theoretically have been made by several investigators.[23–26] Pearson and Matovich[23] carried out a linearized stability analysis of Newtonian fluids subject to isothermal spinning conditions. Shah and Pearson[24] extended the earlier work of Pearson and Matovich by considering a Newtonian fluid and also a power-law fluid subject to nonisothermal spinning. Using the second-order fluid model, Pearson and Matovich[23] have speculated that fluid elasticity would stabilize the resonant behavior of molten threadlines. Using a generalized Maxwell fluid model, Zeichner et al.[25] have made an analysis of the stability of a threadline under stretching and reached the conclusion that the fluid elasticity stabilizes the flow.

More recently, based on their theoretical study, Fisher and Denn[27] presented the view that the occurrence of draw resonance has nothing to do with the fluid elasticity, because even Newtonian fluids can exhibit the phenomenon of draw resonance at a critical stretch ratio of about 20, as was also predicted earlier by Pearson and Matovich.[23]

However, as may be seen in Figures 10 and 11, the onset of draw resonance in the spinning of viscoelastic polypropylene melts can indeed occur at stretch ratios much lower than the value of 20 predicted theoretically for Newtonian fluids, depending on the shear deformation history that the fluid experienced and on the melt temperature. Moreover, the onset of draw resonance can also be affected by the way cooling occurs, as may be seen in Figure 12. The experimental results presented above clearly indicate that fluid elasticity (more precisely stated, the amount of recoverable elastic strain in a fluid exiting from a die) tends to make the thread more unstable, an observation which is opposite to some of the theoretical predictions.[23–26] In other

words, fluid elasticity plays an important role in the occurrence of draw resonance and it indeed tends to *destabilize* the elongational flow behavior of viscoelastic fluids. The Weissenberg number $\lambda V/L$ might be a convenient parameter for correlating a critical stretch ratio to fluid elasticity and processing conditions. Here λ is the relaxation time of a fluid, V a characteristic velocity, and L a characteristic length.

It should be remembered that, once draw resonance occurs, two things go against the production of acceptable fibers: one is the unevenness of the threadlines (i.e., denier variations may be larger than the acceptable level), and the other is the enhanced possibility of breakage of the threadlines. Thus, a very practical and important question may be raised: how can one stretch threadlines fast without having draw resonance?

The present study suggests a number of approaches one can take to avoid draw resonance. They are (1) design the shape of the spinnerette hole to reduce die swell (i.e., larger L/D ratio, smaller D_R/D ratio, and smaller entrance angle α will be helpful); (2) increase the melt temperature; and (3) provide *delayed* quench, i.e., let the molten threadlines first relax in a heated environment upon exiting from the spinnerette holes and then cool them. In reality, it may not be possible for one to have all the choices suggested above. However, any one of the suggestions made above (or any combination thereof) will help to produce fibers having less denier variation *if* the variation arises from the occurrence of draw resonance.

However, further theoretical and experimental studies are needed for a better understanding of the role of fluid elasticity in the resonant behavior of viscoelastic polymer melts. Future experimental study should be concerned with correlating the onset of draw resonance with the molecular structure of a polymer and also with the structural formation of a fiber. Future theoretical study should give consideration to determining more precisely the role of fluid elasticity in the occurrence of draw resonance.

The authors are grateful for the financial support received from American Enka Company.

References

1. E. B. Bagley, S. H. Storey, and D. C. West, *J. Appl. Polym. Sci.*, **7**, 1661 (1963).
2. N. Nakajima and M. Shida, *Trans. Soc. Rheol.*, **10**, 299 (1966).
3. C. McLuckie and M. G. Rogers, *J. Appl. Polym. Sci.*, **13**, 1046 (1969).
4. C. D. Han, M. Charles, and W. Philippoff, *Trans. Soc. Rheol.*, **14**, 393 (1970).
5. R. Kowalski, Ph.D. Dissertation (Ch.E.), Polytechnic Institute of Brooklyn, Brooklyn, N.Y., 1963.
6. C. D. Han and K. U. Kim, *Polym. Eng. Sci.*, **11**, 395 (1972).
7. D. Poller and O. L. Reedy, *Mod. Plast.*, **41** (3), 133 (1964).
8. C. D. Han, *J. Appl. Polym. Sci.*, **17**, 1403 (1973).
9. M. Zidan, *Rheol. Acta*, **8**, 89 (1969).
10. C. D. Han and L. Segal, *J. Appl. Polym. Sci.*, **14**, 2973 (1970).
11. D. Acierno, J. N. Dalton, J. M. Rodriguez, and J. L. White, *J. Appl. Polym. Sci.*, **15**, 2395 (1971).
12. C. D. Han and R. R. Lamonte, *Trans. Soc. Rheol.*, **16**, 447 (1972).
13. I. Chen, G. E. Hagler, L. E. Abbott, J. N. Dalton, D. C. Bogue, and J. L. White, *Trans. Soc. Rheol.*, **16**, 473 (1972).
14. J. A. Spearot and A. B. Metzner, *Trans. Soc. Rheol.*, **16**, 495 (1972).
15. C. D. Han and Y. W. Kim, *J. Appl. Polym. Sci.*, **18**, 2589 (1974).
16. C. D. Han, R. R. Lamonte, and Y. T. Shah, *J. Appl. Polym. Sci.*, **16**, 3307 (1972).

17. J. C. Miller, *SPE Trans.*, **3**, 134 (1963).
18. H. I. Freeman and M. J. Coplan, *J. Appl. Polym. Sci.*, **8**, 2389 (1964).
19. A. Bergonzoni and A. J. DiCresce, *Polym. Eng. Sci.*, **6**, 45 (1966).
20. M. E. Morrison, private communications, 1974.
21. J. Zimmerman, private communications, 1975.
22. C. D. Han and K. Funatsu, unpublished research, 1974.
23. J. R. A. Pearson and M. A. Matovich, *Ind. Chem. Eng. Fundam.*, **8**, 605 (1969).
24. Y. T. Shah and J. R. A. Pearson, *Ind. Chem. Eng. Fundam.*, **11**, 145 (1972).
25. G. R. Zeichner, B. E. Anshus, M. M. Denn, and A. B. Metzner, paper presented at the 44th Annual Meeting of the Society of Rheology, Montreal, Canada, October 28–31,1973.
26. S. Kase, *J. Appl. Polym. Sci.*, **18**, 3279 (1974).
27. R. J. Fisher and M. M. Denn, paper presented at the 159th National Meeting of ACS, Philadelphia, Pa., April 6–11, 1975.

Received July 7, 1975
Revised August 13, 1975